EGH422: Advanced Thermodynamics

Lab Report

Group Members		Contribution
Jacob Garcia-Pavy	N10012478	100%

1.0 Introduction

Heat exchangers are vital, used to transfer heat from one place to another through one medium to another. Effectiveness of a heat exchanger relies on three important parameters. Firstly, the overall heat transfer coefficient. Secondly, the physical size. Thirdly, the total weight. With size and weight being restricted by space and practicality. Overall heat transfer coefficient is the most desirable parameter. Heat exchangers transfer heat from one fluid to a separating boundary and then from the separating boundary to another fluid through conduction, convection, and radiation [1]. However, radiation can be ignored within this situation having little affect with insignificant temperature differences. Heat exchangers come in various configurations which will be examined through this lab report.

2.0 Objectives

This lab report has several objectives. This paper aims to determine the relationship between volumetric flow rate and heat transfer. Furthermore, analyse several types of heat exchangers to establish differences for potential advantages and disadvantages. In addition, aims to validate and compare computational with experimental results. Which will be achieved by obtaining the average temperature difference (LMTD), heat transfer area and the heat transfer coefficient.

3.0 Methodology

3.1 Computational Method

ANSYS Fluent was used to simulate an Aluminium Double Pipe and Copper Double Pipe heat exchanger in parallel and counter flow. The computational method follows:

Geometry

Two geometries were created in DesignModeler to represent respectively the aluminium and copper heat exchangers. The geometries assume the outer pipe is fully insulated being adiabatic thus the outermost wall can be ignored. Both geometries share the same outer diameters of 15.8mm and 19.94mm, however the inner diameters differ being 12.6mm and 13.84mm for the aluminium and copper pipes respectively.

Mesh

All mesh methods were tested to identify the most appropriate and best quality mesh. Most notably the default, automatic and sweep methods produced similar meshes and number of nodes. While the tetrahedral and multizone methods shared the lowest number of nodes. The multizone method generated the worst quality mesh. However, this was significantly

improved by applying a hexa-base which is seen in figure 1. This still produced a poor inner pipe mesh seen in figure 2, which is detrimental as the inner pipe mesh displays significant data thus requiring a high-quality mesh. The tetrahedral method generated the most favourable mesh having considerably more blue elements and less low rated colours seen in figure 3 and 4. However, the method lacked refinement strategies. Consequently, the default method was chosen with element sizing to further refine the mesh seen in figure 5. While the inner pipe was meshed with the tetrahedral method being the most consistent and favourable mesh seen in figure 6.

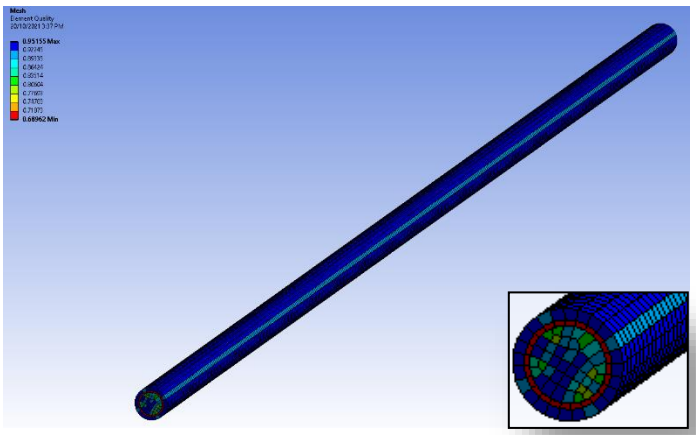

Figure 1, Multizone Mesh (Hexa Free mesh)

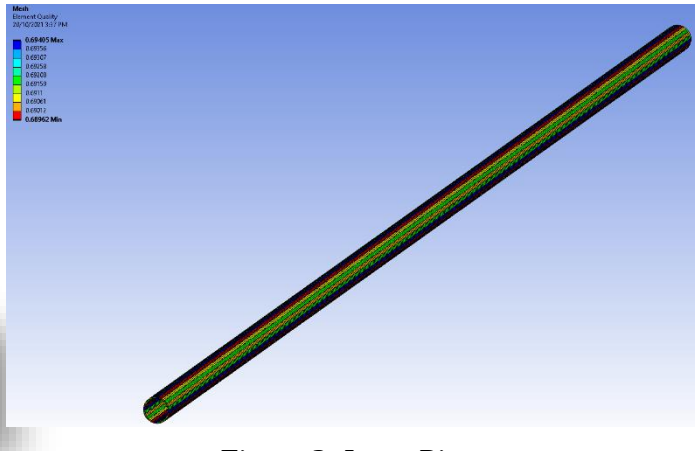

Figure 2, Inner Pipe

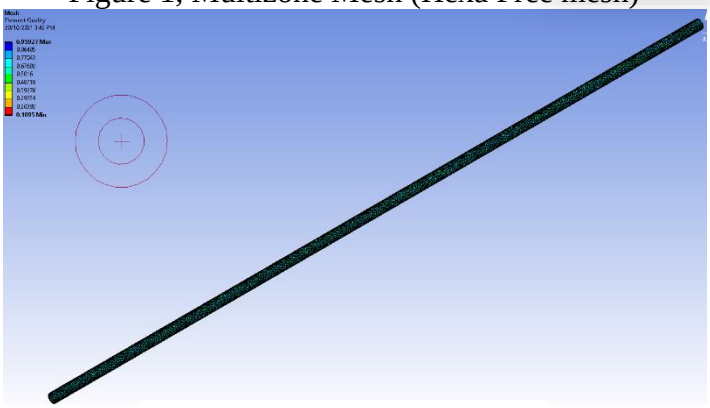

Figure 3, Tetrahedral Mesh

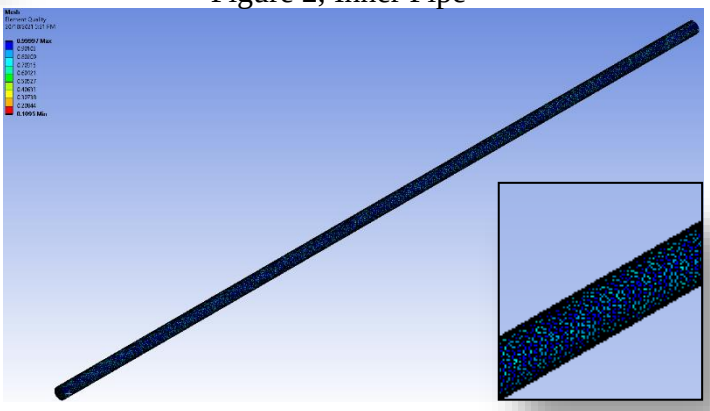

Figure 4, Inner Pipe

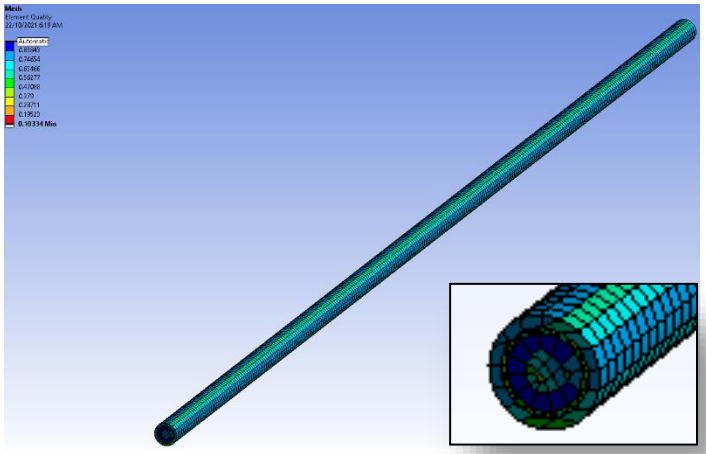

Figure 5, Selected Mesh

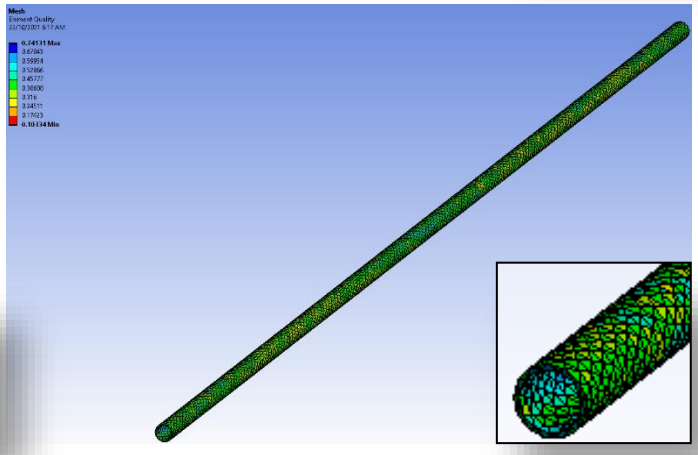

Figure 6, Inner Pipe

The element size started at 4mm and was iteratively reduced until an appropriate size. 2mm was concluded to calculate the most optimal results. The mesh can be seen in figure 7. It had a low computational time while reducing variation seen in table 1. Further refinement proved to exponentially increase computational time with little variation.

Element Size	Nodes	Inlet Temperatures		Difference	
		Hot	Cold		
4mm	26703	322.238	296.452	-	-
3mm	42734	322.032	296.584	-.206	.132
2mm	97680	322.153	296.638	.121	.054

Table 1, Mesh Refinement Strategy

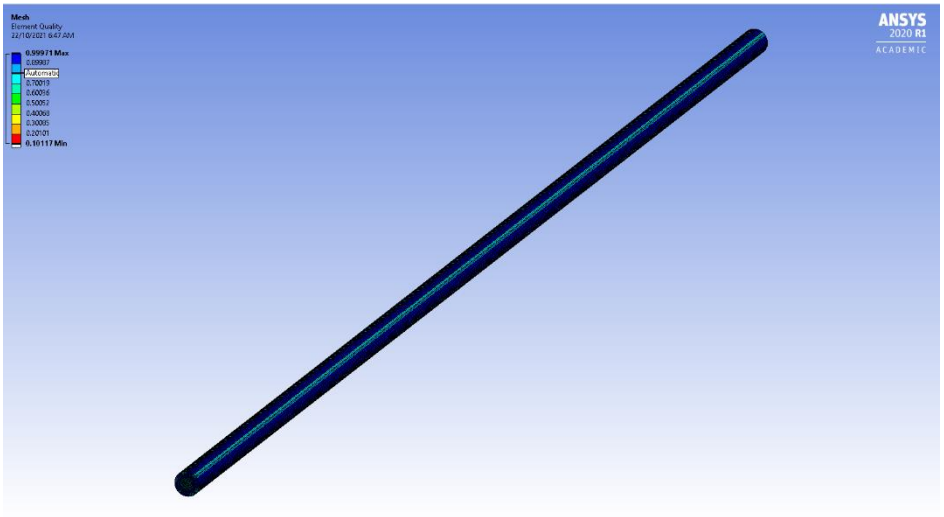

Figure 7, Refined Mesh

Setup

There was specific reasoning for decisions and boundary conditions chosen in the setup. The lowest Reynolds number was calculated to be vicious, thus the k-epsilon was chosen as a widely used 2 equation model. Materials were selected with specific values including the thermal conductivity using the same values seen in table 5. The boundary conditions were set for the respective cases. For parallel flow both inlets were set as mass flow inlets with the respective mass flow rate and temperature presented in table 2. While the outlets were set as default pressure outlets. To simulate counter flow the inlet and outlet were reversed. Thus, the inlet was set to a pressure outlet and the outlet was set to a mass flow rate inlet. Simulations were initialised to test convergence and calculated on 1e-6 residual error and max number of 500 iterations to assure accurate and quick results. Mesh methods such as sweep didn't converge upon initialisation which followed with long and strenuous computational times with lower accuracy.

Results

The results were setup to easily capture the velocity and temperature contours across the pipe. Also, the outlet temperatures and inlet temperatures for respective parallel and counter flow heat exchangers. Which was used to calculate the Logarithmic Mean Temperature Difference (LMTD), the heat transfer and coefficient.

3.2 Experiment Method

Data was recorded within the allotted laboratory using the HAMPDEN Model H-6878 6-Pass Heat Exchanger Demonstrator. Which includes the aluminium and copper heat exchangers in parallel and counter flow through the manipulation of valves. In addition, housed the shell and tube and cross flow heat exchangers. Volumetric flow rate was controlled via a valve. The values were calculated through the instrument through a built-in feature, however, the values were prone to fluctuations thus stabilisation was ensured by the members to gather accurate results.

4.0 Observations

4.1 Computational Simulations

Mass flow rate has been introduced into table 2 and 3 for ease of use, however, is not explicitly calculated or mentioned until required in sections 5.3 later in the report.

Case No.	Heat Exchanger Type	Simulation No.	Volume Flow Rate (Litres/Min)		Mass Flow Rate Inlet (kg/s)		Inlet Temperature ($°C$)		Outlet Temperature ($°C$)	
			Hot	Cold	Hot	Cold	Hot	Cold	Hot	Cold
1	Aluminium Parallel Flow	1a	5.6	4.2	0.091974955	0.069941813	54.1	13.5	46.661	23.438
		1b	10.8	8.4	0.177331356	0.139845188	54.6	15.4	47.973	23.956
		1c	16	12.2	0.262386347	0.20308607	56.8	16.1	50.366	24.577
		1d	21.6	16.8	0.354915198	0.279719874	53.3	14.7	47.441	22.289
2	Aluminium Counter Flow	2	21	16.8	0.34500032	0.279748	53.6	14	47.428	21.81
3	Copper Parallel Flow	3	22	16.8	0.361150167	0.279668466	55	15.9	49.153	23.638
4	Copper Counter Flow	4	21	16.8	0.34450073	0.279631954	56.2	16.7	50.131	24.421

Table 2, Computational Simulations

4.2 Experimental Results

Case No.	Heat Exchanger Type	Simulation No.	Volume Flow Rate (Litres/Min)		Mass Flow Rate Inlet (kg/s)		Inlet Temperature ($°C$)		Outlet Temperature ($°C$)	
			Hot	Cold	Hot	Cold	Hot	Cold	Hot	Cold
1	Aluminium Parallel Flow	1A	5.6	4.2	0.091974955	0.069941813	54.1	13.5	38	27
		1B	10.8	8.4	0.177331356	0.139845188	54.6	15.4	40.2	23.8
		1C	16	12.2	0.262386347	0.20308607	56.8	16.1	42.7	24.8
		1D	21.6	16.8	0.354915198	0.279719874	53.3	14.7	41.2	23.2
2	Aluminium Counter Flow	2	21	16.8	0.34500032	0.279748	53.6	14	43	25.4
3	Copper Parallel Flow	3	22	16.8	0.361150167	0.279668466	55	15.9	45.4	21.8
4	Copper Counter Flow	4	21	16.8	0.34450073	0.279631954	56.2	16.7	48	24.2
5	Shell and Tube Heat Exchanger	5A	10.4	8.6	0.17067765	0.143156718	55.5	16.2	37.5	23.3
		5B	21.6	17	0.354857472	0.282912173	53.6	17.7	43.7	23.1
6	Cross Flow Heat Exchanger	6A	10.6	8.6	0.174133541	0.143179221	53.7	13.5	33	24.4
		6B	21.8	16.8	0.358259383	0.279723976	53	15.4	31.2	22

Table 3, Experimental Results

5. Calculations, Analysis & Results

5.1 Logarithmic Mean Temperature Difference (LMTD)

(a) Computational and Experimental example calculation.

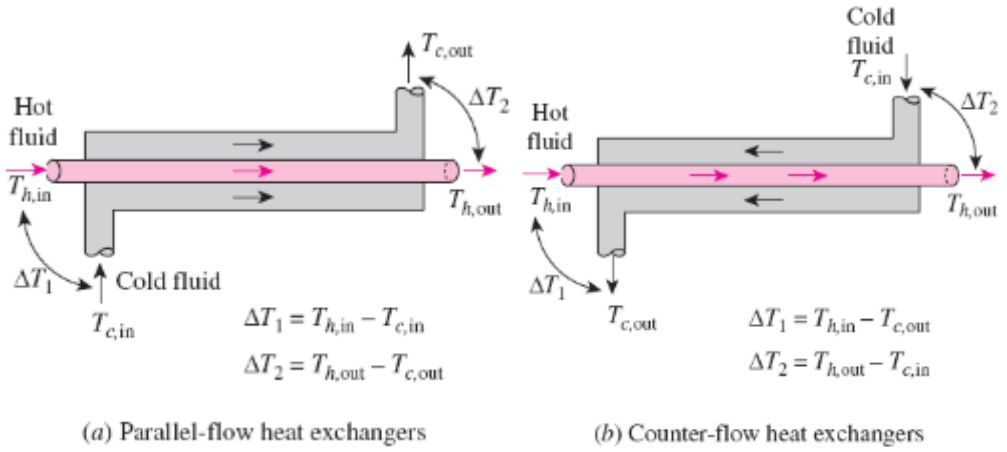

Figure 8, Parallel and Counter Flow LMTD

$$LMTD = \Delta T_{ln} = \frac{\Delta T_1 - \Delta T_2}{\ln(\Delta T_1 / \Delta T_2)} \dots (1)$$

Computational Calculation- [Simulation No.1a (Parallel Flow)]	**Experimental Calculation- [Simulation No.1A (Parallel Flow)]**
The required equations for parallel flow are $\Delta T_1 = T_{h,in} - T_{c,in} \dots (2)$ $\Delta T_2 = T_{h,out} - T_{c,out} \dots (3)$	
Where $T_{h,in} = 54.1, T_{h,out} = 46.661$ $T_{c,in} = 13.5, T_{c,out} = 23.438\ (°C)$	Where $T_{h,in} = 54.1, T_{h,out} = 38, T_{c,in} = 13.5, T_{c,out} = 27\ (°C)$
$\Delta T_1 = 54.1 - 13.5 \dots (2)$ $\Delta T_1 = 40.6°C$	$\Delta T_1 = 54.1 - 13.5 \dots (2)$ $\Delta T_1 = 40.6°C$
$\Delta T_2 = 46.661 - 23.438 \dots (3)$ $\Delta T_2 = 23.223°C$	$\Delta T_2 = 38 - 27 \dots (3)$ $\Delta T_2 = 11°C$
Subbing into equation (1)	*Subbing into equation* (1)
$\Delta T_{ln} = \frac{40.6 - 23.23}{\ln\left(\frac{40.6}{23.23}\right)} \dots (1)$ $\Delta T_{ln} = 31.107$	$\Delta T_{ln} = \frac{40.6 - 11}{\ln\left(\frac{40.6}{11}\right)} \dots (1)$ $\Delta T_{ln} = 22.67$

Excel was used to calculate all the LMTD values seen in table 4 with the respective formula and method for each type of heat exchanger.

b) Computational and Experimental LMTD

Heat Exchanger Type	Simulation No.	LMTD	
		Experiment	Computational Analysis
Aluminium Parallel Flow	1A	22.66683	31.10674087
	1B	26.16493	30.9911008
	1C	27.75656	32.67949161
	1D	27.00292	31.39746306
Aluminium Counter Flow	2	28.59814	32.60214224
Copper Parallel Flow	3	30.70062	35.08891293
Copper Counter Flow	4	31.64871	32.59802364
Shell and Tube Heat Exchanger	5A	26.37569	NA
	5B	28.19016	
Cross Flow Heat Exchanger	6A	23.07434	
	6B	23.05533	

Table 4, Computational and Experimental LMTD

(c) Comparison of LMTD for Experiment and Computational analysis

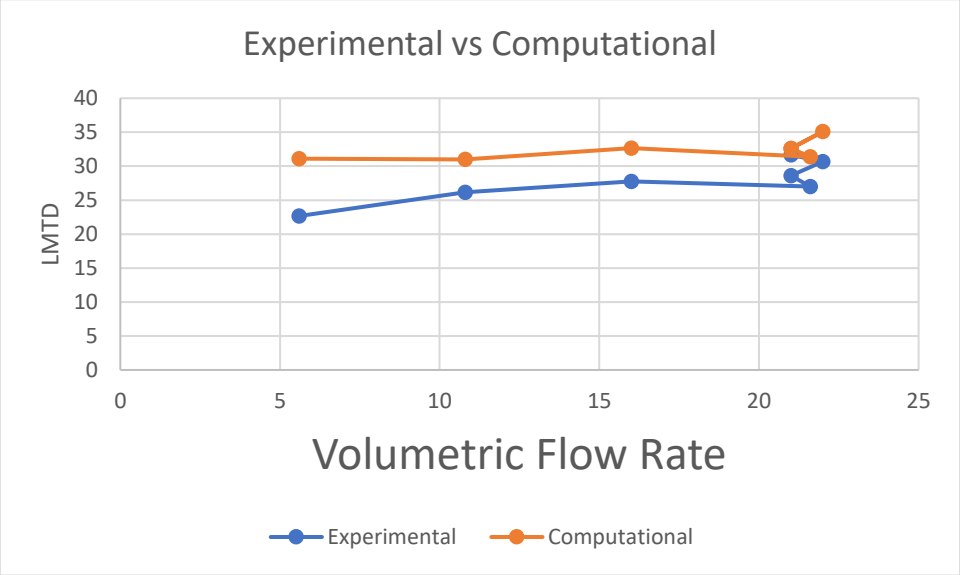

Figure 9, Experimental LMTD vs Computational LMTD

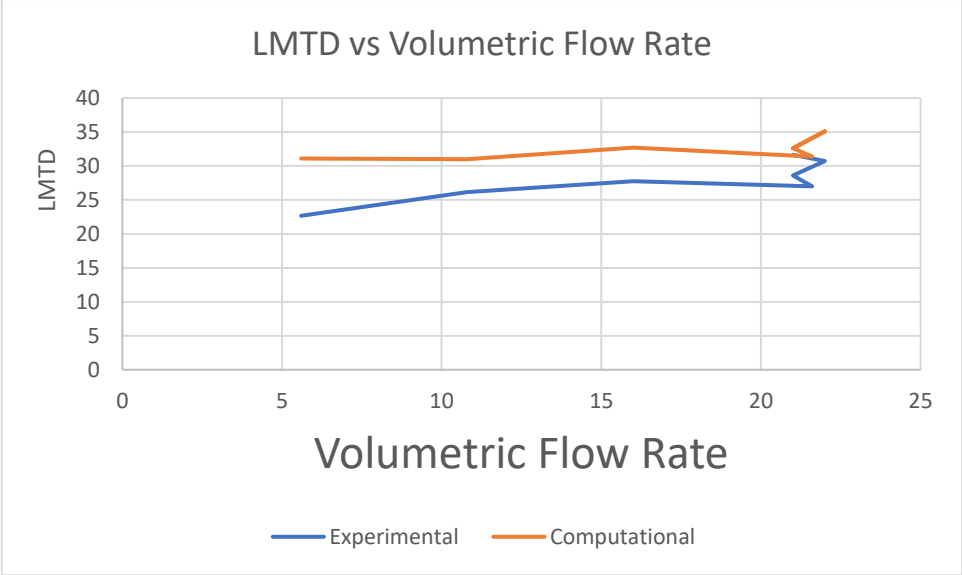

Figure 10, LMTD vs Volumetric Flow Rate

5.2 Heat Transfer Areas

a) Computational and Experimental Analysis

The computational and experimental values were concluded to be the same. The diameters and conductivity were share specified values while the calculated areas do not significantly differ.

Heat Exchanger Type	No. of Tubes	Length (m)	Inner Pipe Diameter (m)	Outer Pipe Diameter (m)	Inner Pipe Surface Area (m^2)	Outer Pipe Surface Area (m^2)	Thermal Conductivity $(W/m \cdot K)$
Aluminium	1	1.21	12.60e-3	15.875e-3	4.79E-02	6.03E-02	154
Copper	1	1.21	13.84e-3	15.875e-3	0.052610367	0.060346068	339
Shell and Tube Heat Exchanger	28	.2	5.52e-3	6.35e-3	0.003468318	0.003989823	339
Cross Flow Heat Exchanger	60	.35	5.6e-3	7e-3	0.006157522	0.007696902	339

Table 5, Heat Transfer Area

5.3 Heat Transfer Coefficients

a) Mass Flow Rate Example Calculation

Mass Flow Rate Formula

$$\dot{m}(\frac{kg}{s}) = \dot{Q}\left(\frac{L}{min}\right) \cdot \frac{1}{1000m^3} \cdot \frac{1}{60s} \cdot p \ldots (4)$$

Density equation regarding Celsius

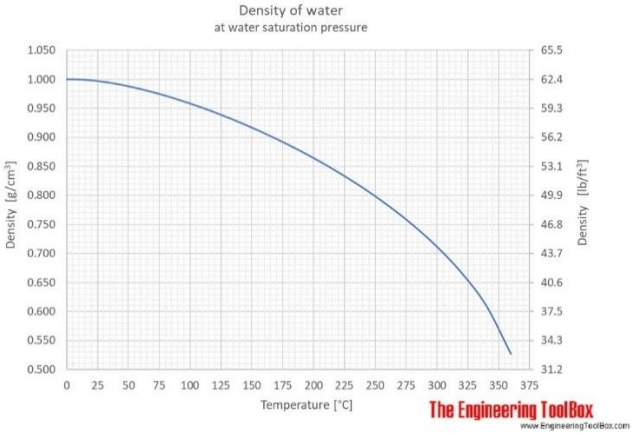

Figure 11, Water Density (g/cm^3) vs Temperature (Celsius) [1]

With the graph above and the condition that water is $1\frac{g}{m^3}$ at 4 $(°C)$ the density equation was approximately determined, equation (5). Calculations are included in appendix B.

$$p\left(\frac{kg}{m^3}\right) = -.005x^2 + 1000.08.. (5)$$

$$Subbing\ into\ equation\ (4)$$

$$\dot{m} = \dot{Q}\left(\frac{L}{min}\right) \cdot \frac{1}{1000m^3} \cdot \frac{1}{60} \cdot -.005x^2 + 1000.08 \ldots (6)$$

$$Where\ x = inlet\ temperature\ for\ respective\ hot\ and\ cold\ fluid$$

Hot Inlet,	**Cold Inlet**
$\dot{Q} = 5.6\left(\frac{L}{min}\right), x = 54.1℃$	$\dot{Q} = 4.2\left(\frac{L}{min}\right), x = 13.5℃$
$\dot{m} = \frac{5.6}{60000} \cdot p \ldots (7)$ $\dot{m} = .000093 \cdot (-.005(54.1)^2 + 1000.08) \ldots (8)$ $\dot{m} = .092\ kg/s$	$\dot{m} = \frac{4.2}{60000} \cdot p \ldots (7)$ $\dot{m} = .00007 \cdot (-.005(13.5)^2 + 1000.08) \ldots (8)$ $\dot{m} = .0699\ kg/s$

Excel was used to quickly calculate the values given in table 6.

b) Calculated Mass Flow Rate, Volumetric Flow Rate and Density

Simulation No.	Mass Flow Rate (kg/s) Inlet		Volume Flow Rate (Litres/Min)		Density(kg/m^3)	
	Hot	Cold	Hot	Cold	Hot	Cold
1A	0.09197496	0.0699418	5.6	4.2	985.446	999.1688
1B	0.17733136	0.1398452	10.8	8.4	985.1742	998.8942
1C	0.26238635	0.2030861	16	12.2	983.9488	998.784

1D	0.3549152	0.2797199	21.6	16.8	985.8756	998.9996
2	0.34500032	0.279748	21	16.8	985.7152	999.1
3	0.36115017	0.2796685	22	16.8	984.955	998.816
4	0.34450073	0.279632	21	16.8	984.2878	998.6856
5A	0.17067765	0.1431567	10.4	8.6	984.6788	998.7678
5B	0.35485747	0.2829122	21.6	17	985.7152	998.5136
6A	0.17413354	0.1431792	10.6	8.6	985.6616	998.9248
6B	0.35825938	0.279724	21.8	16.8	986.035	999.0142

Table 6, Calculated Mass Flow Rate, Volumetric Flow Rate and Density

c) Heat Transfer Coefficient (HTC) Example Calculation

$$Q = \dot{m} \cdot C_p \cdot \Delta T \ldots (9)$$

$$U = \frac{Q}{LMTD \cdot A} \ldots (10)$$

For simulation case 1a

Simulation Case 1a	
Hot Fluid	Cold Fluid
$\dot{m} = .092\frac{kg}{s}, \Delta T_h = -7.439K$ $C_p \approx 4.18kJ/WK$ $LMTD = 31.107\,, A_h = 4.79e-2$	$\dot{m} = .07\ kg/s, \Delta T_c = 9.938K$ $C_p \approx 4.18kJ/WK$ $LMTD = 31.107, A_h = 6.03e-2$
$Q_h = .092 \cdot 4.18 \cdot -7.439 \ldots (9)$ $Q_h = -2.86kW$ $U = \frac{-2.86}{31.107 \cdot 4.79e-2} \ldots (10)$ $U = -1.92kW/m^2K$	$Q_c = .07 \cdot 4.18 \cdot 9.938 \ldots (9)$ $Q_c = 2.907kW$ $U = \frac{2.907}{31.107 \cdot 6.03e-2} \ldots (10)$ $U = 1.55kW/m^2K$

d) Calculated HTC

Computational

Simulation No.	Temperature Difference (K/℃)		Heat lost (kW)		Heat Transfer Coefficient (kW/m^2K)	
	Hot	Cold	Hot	Cold	Hot	Cold
1a	-7.439	9.938	-2.85996	2.905442	-1.92E+00	1.55E+00
1b	-6.627	8.556	-4.91223	5.001434	-3.30907	2.676334
1c	-6.434	8.477	-7.05665	7.196123	-4.50804	3.651792
1d	-5.859	7.589	-8.69209	8.873279	-5.77955	4.686755
2	-6.172	7.81	-8.90065	9.132597	-5.69954	4.645483
3	-5.847	7.738	-8.82668	9.045832	-5.2516	4.275248
4	-7.439	9.938	-8.73944	9.02478	-5.59702	4.591219

Table 7, Calculated computational Heat Transfer and coefficient

Experimental

Simulation No.	Temperature Difference (K/°C)		Heat lost (kW)		Heat Transfer Coefficient (kW/m^2K)	
	Hot	Cold	Hot	Cold	Hot	Cold
1A	-16.1	13.5	-6.18973	3.946816	-5.70E+00	2.89E+00
1B	-14.4	8.4	-10.6739	4.910244	-8.51666	3.11219073
1C	-14.1	8.7	-15.4645	7.385428	-11.6315	4.412580942
1D	-12.1	8.5	-17.9509	9.938447	-13.8784	6.10366267
2	-10.6	11.4	-15.2863	13.33055	-11.1591	7.730242139
3	-9.6	5.9	-14.4922	6.897184	-9.85491	3.725695
4	-8.2	7.5	-11.8081	8.766462	-7.78913	4.593577207
5A	-18	7.1	-12.8418	4.248605	-10.1645	2.671316049
5B	-9.9	5.4	-14.6847	6.385894	-10.8751	3.756702113
6A	-20.7	9.2	-15.0671	5.5061	-13.6321	3.957286126
6B	-21.8	7.4	-32.646	8.652422	-29.5613	6.223706426

Table 8, Calculated experimental Heat Transfer and coefficient

e) Compare Results for computation and experiments

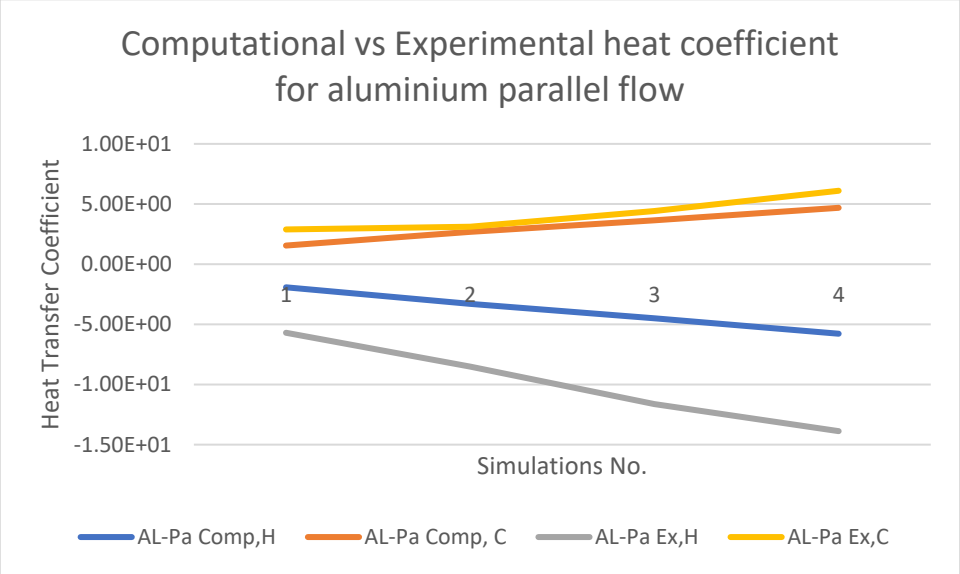

Figure 11, Computational vs Experimental Heat transfer coefficient for aluminium parallel flow

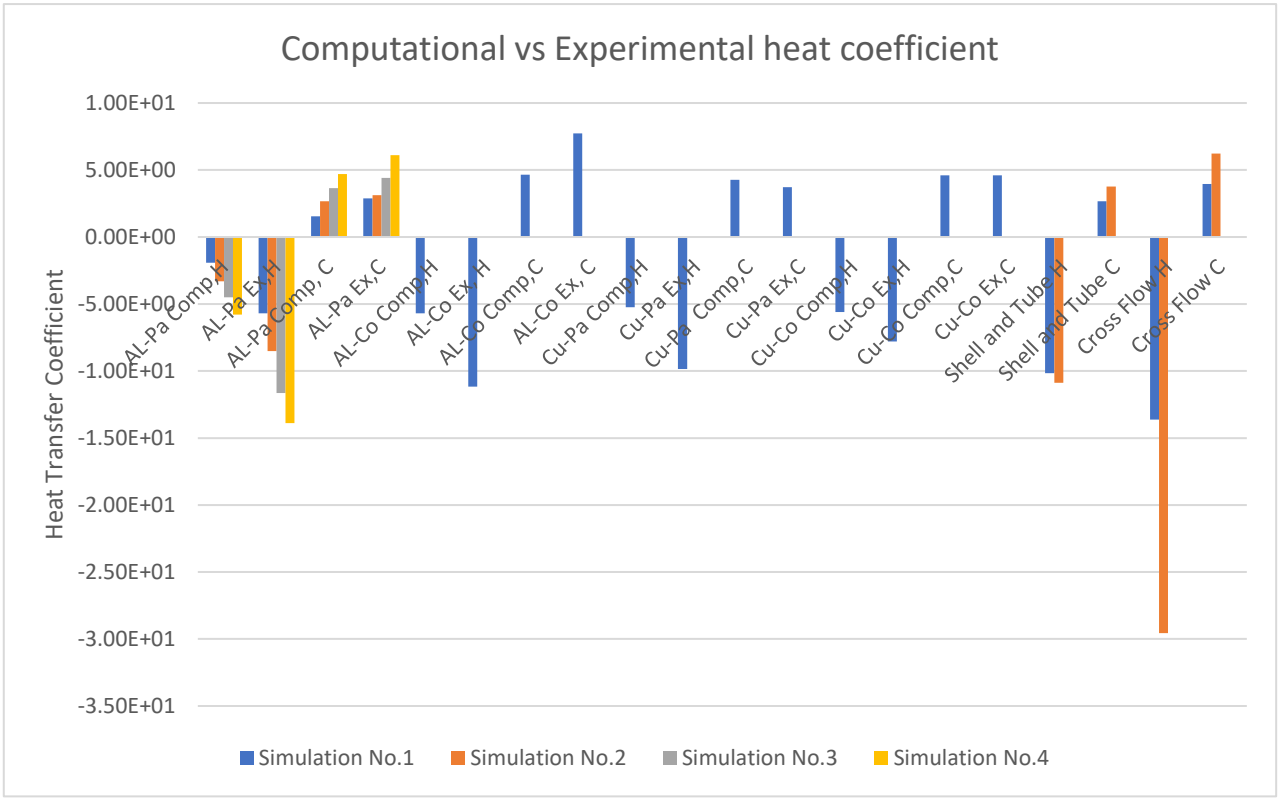

Figure 12, Computational vs Experimental Heat Transfer Coefficient

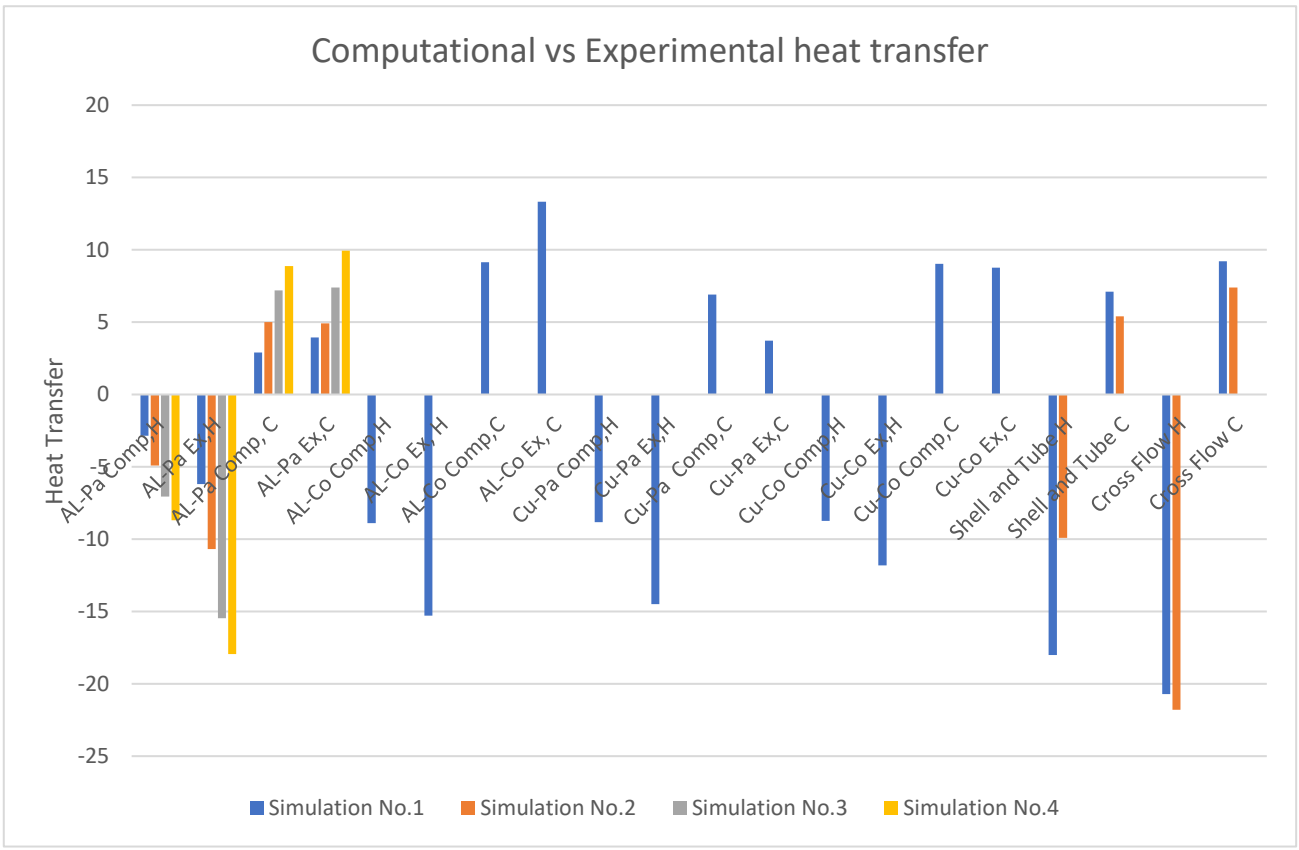

Figure 13, Computational vs Experimental Heat Coefficient Transfer

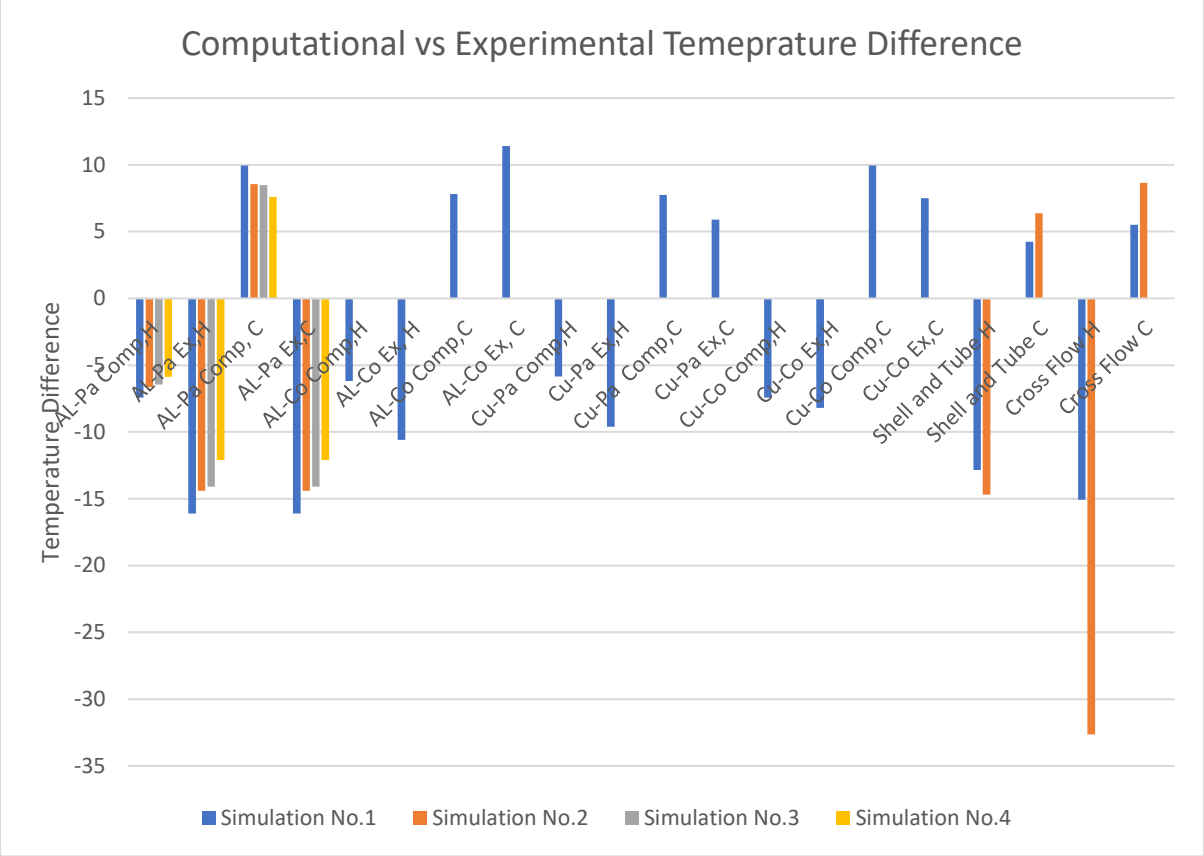

Figure 14, Computational vs Experimental Temperature Difference

6.0 Discussion

The initial computational and experimental findings presented in section 4 displays the respective temperature readings regarding the inlet and outlet of the hot and cold fluid of the heat exchangers. Moreover, it includes the volumetric flow rate and introduces the mass flow rate, however, was not specified or necessary at that stage. The simulation conveys several limiting factors. There was a significant time constraint placed on the simulations as the report was conducted individually. More simulations for the Aluminium Counter Flow, Copper Parallel Flow and Copper Counter Flow with varying volumetric flow rate like the Aluminium Parallel Flow simulations would've allowed greater and stronger findings. Similarly, optimal meshes were selected to reduce computational time and power instead of higher quality meshes which introduces slight inaccuracies within the simulation. Furthermore, the outermost wall was assumed adiabatic thus it was ignored within the geometry which isn't portrayed within the experiment. Overall, the simulated results contain several limitations which weakens its significance.

Section 5.1 displays the calculated computational and experimental LMTD which were compared through several plots. The orange line series seen in figure 9 shows that the computational LMTD closely resembles experimental LMTD denoted by the blue line series. Overall, following a similar trend though slightly inflated. This may be caused by potential fouling factor of the experimental equipment which deteriorates heat exchanger performance. Accumulations of deposits on heat transfer surfaces increases the thermal resistance which leads to a decrease in heat transfer coefficient and energy, thus reducing LMTD.

Figure 10 displays a distinct correlation between volumetric flow rate and LMTD. Larger volumetric flow rate was concluded to generate greater LMTD values which was hypothesised. Volumetric flow rate and mass flow rate can be correlated through unit conversion which is seen through calculations in section 5.1. Mass flow rate is one of three dependent variables in the energy equation (9) thus volumetric flow rate theoretically influences heat transfer coefficient and energy, consequently LMTD. The calculations presented in section 5.1 display a strong limitation regarding the approximation of the density equation. Which is utilised in all proceeding calculations and results. However, is insignificant as the density values do not drastically defer from the reference values.

The experimental and computational results seen in table 4 display inverse relationships with counter and parallel flow. Experimental data display an increase in LMTD with counter flow, however, a decrease in LMTD in the computational data. The difference is quite negligible and may be underlined by limited simulations.

Figure 11 displays the computational and experimental heat transfer coefficient for the hot and cold fluid for each aluminium parallel flow simulation. There is strong connection between the computational and experimental heat transfer coefficient for the cold fluid. However, the hot fluid seems to have large discrepancies. Despite this, both the computational and experimental display appropriate behaviours. The hot and cold fluid increases heat transfer rate as following simulations increases volumetric flow rate. In addition, it is expected that the hot fluid has a negative heat transfer coefficient losing heat, while the cold fluid has a positive heat transfer coefficient gaining the respective heat.

Figure 12, 13 and 14 displays respectively the heat transfer coefficient, overall heat transfer and temperature difference. Figures 12 and 13 corroborates the correlation between volumetric flow rate and heat transfer. The iterative volumetric flow rate for the aluminium parallel flow increases both the heat transfer and coefficient. In addition, a notable observation is that the aluminium experimental results are significantly larger than computational results, however, isn’t strongly conveyed for copper. Furthermore, the crossflow heat exchanger appears to generate the greatest heat transfer and coefficient followed by the shell and tube heat exchanger. Which is supported by figure 14 which displays the dramatic temperature difference for the respective heat exchangers proving this variable’s significant in heat transfer. Moreover, the temperature difference noticeably decreasing as volumetric flow rate increases seen in the aluminium parallel flow.

7.0 Conclusion

In conclusion, the experimental results and theory support the computational results with minor discrepancies introduced through several limitations. Time and computational constraints limited the depth and quality of the simulation. While several approximations and assumptions made during the simulation and proceeding calculations are inaccurate, however, insignificant. Fouling factor within the experimental equipment may contribute to the significant disparity between the hot fluid computational and experimental results. Furthermore, the results display a positive relation between volumetric flow rate and subsequent mass flow rate, with Logarithmic Mean Temperature Difference (LMTD), heat transfer and heat transfer coefficient. While the temperature difference is inversely proportional to the volumetric flow rate. Moreover, the crossflow heat exchanger appears to produce the most favourable heat transfer, followed by the shell and tube heat exchanger.

References

[1] "Water - Density, Specific Weight and Thermal Expansion Coefficients", *Engineeringtoolbox.com*, 2021. [Online]. Available: https://www.engineeringtoolbox.com/water-density-specific-weight-d_595.html. [Accessed: 22- Oct- 2021].

Appendix A

1a

1b


Velocity
Contour Velocity
1.691e+00
1.597e+00
1.503e+00
1.409e+00
1.315e+00
1.221e+00
1.128e+00
1.034e+00
9.396e-01
8.456e-01
7.517e-01
6.577e-01
5.638e-01
4.698e-01
3.758e-01
2.819e-01
1.879e-01
9.396e-02
0.000e+00
[m s^-1]

1c


Temperature
Contour 1
3.283e+02
3.261e+02
3.239e+02
3.218e+02
3.196e+02
3.174e+02
3.152e+02
3.131e+02
3.109e+02
3.087e+02
3.065e+02
3.043e+02
3.022e+02
3.000e+02
2.978e+02
2.956e+02
2.935e+02
2.913e+02
2.891e+02
[K]


Velocity
Contour Velocity
2.497e+00
2.358e+00
2.219e+00
2.081e+00
1.942e+00
1.803e+00
1.665e+00
1.526e+00
1.387e+00
1.248e+00
1.110e+00
9.710e-01
8.323e-01
6.936e-01
5.549e-01
4.161e-01
2.774e-01
1.387e-01
0.000e+00
[m s^-1]

1d

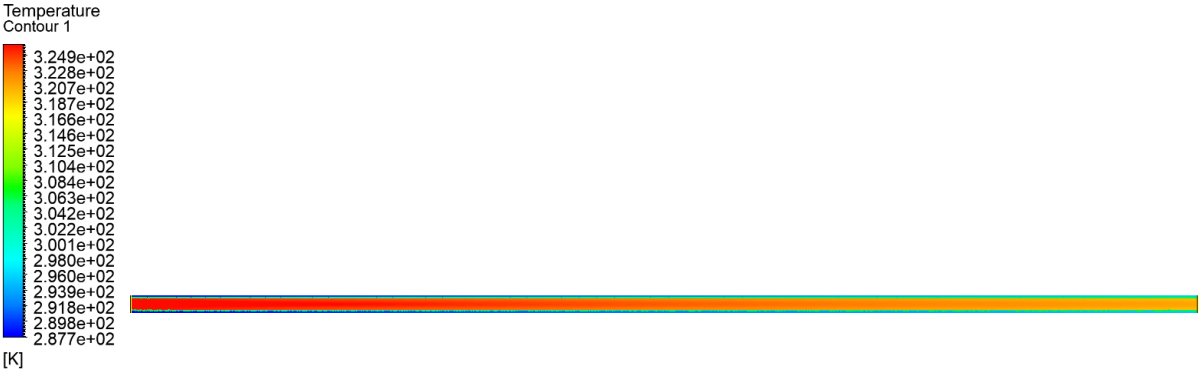
Temperature
Contour 1
3.249e+02
3.228e+02
3.207e+02
3.187e+02
3.166e+02
3.146e+02
3.125e+02
3.104e+02
3.084e+02
3.063e+02
3.042e+02
3.022e+02
3.001e+02
2.980e+02
2.960e+02
2.939e+02
2.918e+02
2.898e+02
2.877e+02
[K]


Velocity
Contour Velocity
3.372e+00
3.184e+00
2.997e+00
2.810e+00
2.622e+00
2.435e+00
2.248e+00
2.060e+00
1.873e+00
1.686e+00
1.499e+00
1.311e+00
1.124e+00
9.366e-01
7.493e-01
5.619e-01
3.746e-01
1.873e-01
0.000e+00
[m s^-1]

2


Temperature
Contour 1
3.251e+02
3.230e+02
3.209e+02
3.188e+02
3.167e+02
3.145e+02
3.124e+02
3.103e+02
3.082e+02
3.061e+02
3.040e+02
3.018e+02
2.997e+02
2.976e+02
2.955e+02
2.934e+02
2.912e+02
2.891e+02
2.870e+02
[K]


Velocity
Contour Velocity
3.278e+00
3.096e+00
2.914e+00
2.732e+00
2.550e+00
2.367e+00
2.185e+00
2.003e+00
1.821e+00
1.639e+00
1.457e+00
1.275e+00
1.093e+00
9.106e-01
7.284e-01
5.463e-01
3.642e-01
1.821e-01
0.000e+00
[m s^-1]

3

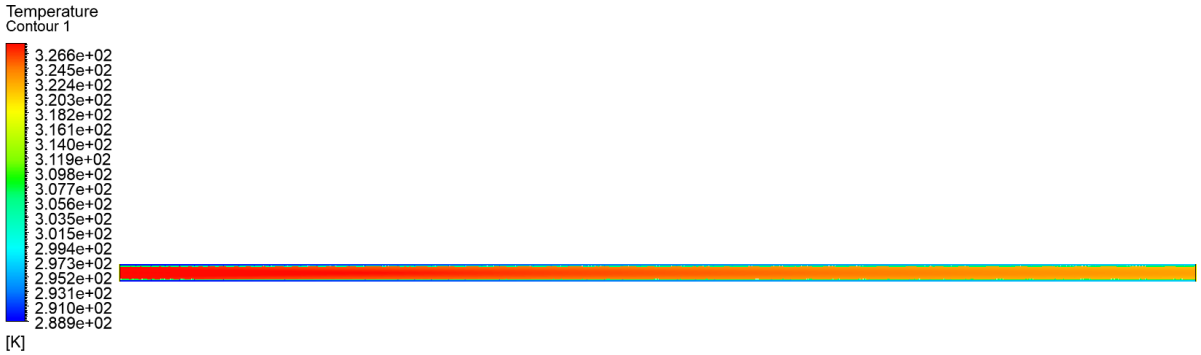
Temperature
Contour 1
3.266e+02
3.245e+02
3.224e+02
3.203e+02
3.182e+02
3.161e+02
3.140e+02
3.119e+02
3.098e+02
3.077e+02
3.056e+02
3.035e+02
3.015e+02
2.994e+02
2.973e+02
2.952e+02
2.931e+02
2.910e+02
2.889e+02
[K]

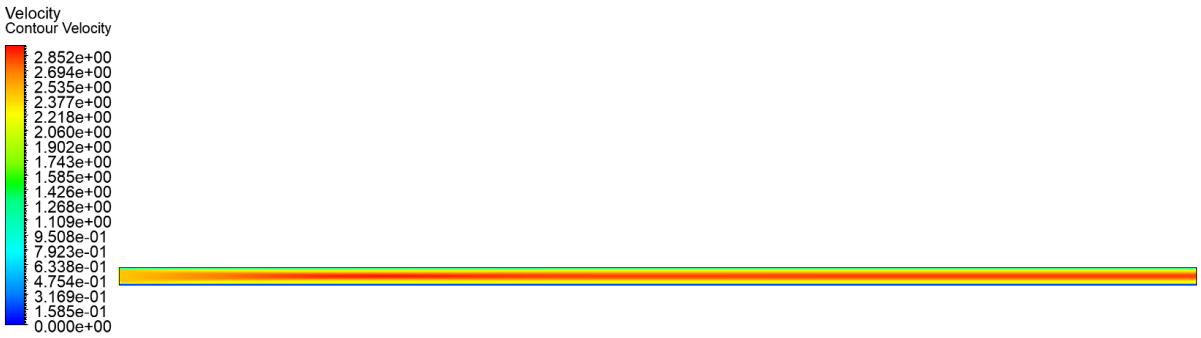
Velocity
Contour Velocity
2.852e+00
2.694e+00
2.535e+00
2.377e+00
2.218e+00
2.060e+00
1.902e+00
1.743e+00
1.585e+00
1.426e+00
1.268e+00
1.109e+00
9.508e-01
7.923e-01
6.338e-01
4.754e-01
3.169e-01
1.585e-01
0.000e+00
[m s^-1]

4

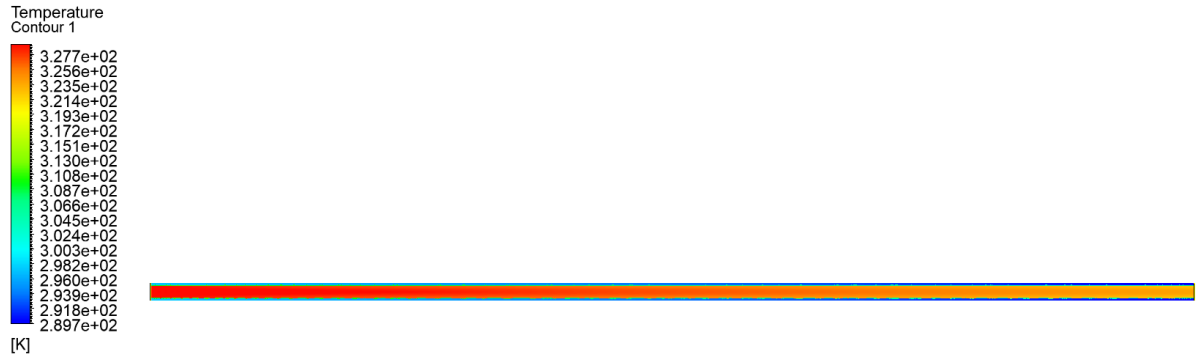
Temperature
Contour 1
3.277e+02
3.256e+02
3.235e+02
3.214e+02
3.193e+02
3.172e+02
3.151e+02
3.130e+02
3.108e+02
3.087e+02
3.066e+02
3.045e+02
3.024e+02
3.003e+02
2.982e+02
2.960e+02
2.939e+02
2.918e+02
2.897e+02
[K]


Velocity
Contour Velocity
2.722e+00
2.570e+00
2.419e+00
2.268e+00
2.117e+00
1.966e+00
1.814e+00
1.663e+00
1.512e+00
1.361e+00
1.210e+00
1.058e+00
9.072e-01
7.560e-01
6.048e-01
4.536e-01
3.024e-01
1.512e-01
0.000e+00
[m s^-1]

Appendix B- Density Formula calculation

$$y = ax^2 + bx + c$$

$\boldsymbol{The\ slope\ of\ the\ function\ is\ zero\ at\ x = 0}$ $\boldsymbol{\dot{y} = 2x + b}$ $\boldsymbol{b = 0}$	$\boldsymbol{at\ x = 4, y = 1}$ $\boldsymbol{1 = 16a + c}$ $\boldsymbol{c = 1 - 16a \ldots (5)}$ $\boldsymbol{at\ x = 80, y = .97}$ $\boldsymbol{.97 = 6400 + c}$ $\boldsymbol{c = .97 - 6400a \ldots (6)}$ $\boldsymbol{Summing\ (5)\ and\ (6)}$ $\boldsymbol{1 - 16a = .97 - 6400a}$ $\boldsymbol{-.03 = 6384a}$ $\boldsymbol{a = -.000005}$	$\boldsymbol{1 - 16a = .97 - 6400a}$ $\boldsymbol{-.03 = 6384a}$ $\boldsymbol{a = -.000005}$ $\boldsymbol{Subbing\ back\ into\ (5)}$ $\boldsymbol{c = 1 - 16(-.000005)}$ $\boldsymbol{c = 1000.08}$

$$Thus\ y\ \left(\frac{g}{m^3}\right) = -.000005x^2 + 1.00008$$

$$Therefore\ y\ (\frac{kg}{m^3}) = -.005x^2 + 1000.08$$